RSC Advances

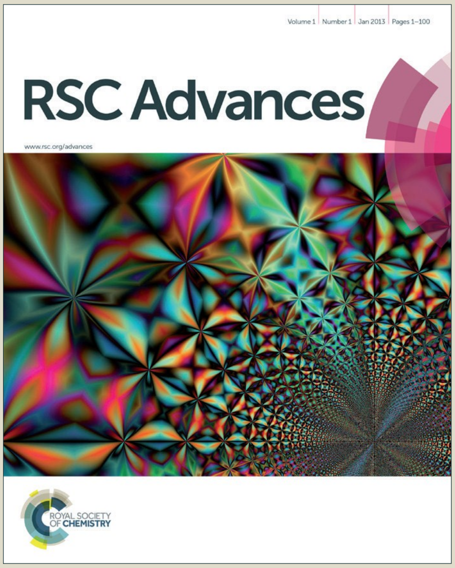

ROYAL SOCIETY OF CHEMISTRY

www.rsc.org/advances

Effect of $CaZrO_3$ on phase structure and electrical properties of KNN-based lead-free ceramics

Yang Zhang[a], Lingyu Li[a], Wangfeng Bai[a], Bo Shen[a], Jiwei Zhai*[a], Bo Li[b]

[a] Key Laboratory of Advanced Civil Engineering Materials of Ministry of Education, Functional Materials Research Laboratory, School of Materials Science & Engineering, Tongji University, 4800 Caoan road, Shanghai 201804, China

[b]Department of Orthopaedics, Yueyang Hospital of Integrated Chinese Medicine and Western Medicine, Shanghai University of Traditional Chinese Medicine, 110 Ganhe Road, Shanghai 200437, China

Abstract: $(1-x)[0.93(K_{0.5}Na_{0.5})NbO_3$-$0.07LiNbO_3]$-$xCaZrO_3$ (KNN-LN-xCZ) lead free piezoelectric ceramics have been prepared by the conventional solid state reaction method and investigated to differentiate the effects of polymorphic phase transition. The crystal structure of ceramics was changed from orthorhombic to tetragonal at $x \geq 0.04$, then both the orthogonal and tetragonal phases coexisted in the region of composition $0.04<x<0.08$ and orthorhombic–tetragonal phase transition were modified to around room temperature. Remarkably piezoelectric and ferroelectric properties has been obtained in KNN-LN-xCZ ternary system with x=0.04, which piezoelectric parameter was d_{33}^* of 320 pm/V, Curie temperature $T_c=350^{o}C$, strain levels of 0.16% at 50 kV/cm and remnant polarization $P_r=27.2\mu C/cm^2$.

***Keywords**:* $(K_{0.5}Na_{0.5})NbO_3$, Piezoelectric, Polymorphic phase transition

---

* Corresponding author. E-mail address: apzhai@tongji.edu.cn.

1. Introduction

PZT-based piezoelectric ceramics have been popularly utilized for several decades for their superior piezoelectric properties.[1,2] However, the high toxicity of lead oxide has caused serious environmental problems. Therefore, there is a great need to develop lead free piezoelectric ceramics with good piezoelectric properties for replacing the lead-based ceramics in various applications.[3-5] Many lead free ferroelectric materials such as barium titanate (BT),[6,7] potassium niobate(KN),[8] potassium sodium niobate(KNN),[9-21] potassium tantalate niobate(KTN)[22-25] and bismuth sodium titanate(BNT),[26-28] have been investigated. Among all the lead free materials, $K_{0.5}Na_{0.5}NbO_3$(KNN), the solid solution of ferroelectric $KNbO_3$ and antiferroelectric $NaNbO_3$, has been studied extensively, considered one of the most promising candidates for lead-free piezoelectric ceramics for its high Curie temperature, outstanding piezoelectric and ferroelectric properties, and large electromechanical coupling coefficients as well as its better environmental compatibility than other lead-free piezoelectric ceramics, which superior piezoelectric attribute to orthorhombic-tetragonal polymorphic phase transition(PPT) around room temperature, and considered to be closely associated with phase coexistence in a way similar to that morphotropic phase boundary (MPB)—a phase boundary that a narrow composition region with orthorhombic or monoclinic phase separating rhombohedral and tetragonal phases in solid solutions—for widely used PZT-based ceramics.[29,30]

However, in contrast to the classical behaviors of nearly temperature-independent MPB, strong piezoelectric temperature dependence is usually observed in KNN-based ceramics with high piezoelectric properties.[22] It was reported that an PPT existed $(1-x)(K_{0.5}Na_{0.5})NbO_3–x(LiNbO_3)$ at about 5–7mol% $LiNbO_3$ and reported excellent piezoelectric properties and high Curie temperature.[31] Yao et al[32] reported $CaZrO_3$ modified KNN-based ceramics, which could reduced lattice distortion and coexistence of orthorhombic and tetragonal phase.

In this work, KNN-LN-xCZ ceramics were prepared by conventional solid state reaction route and the influence of $CaZrO_3$ on the crystal structure and electrical properties of the ceramics were investigated. $LiNbO_3$ was expected to enhance the piezoelectric properties of KNN ceramics. $CaZrO_3$ was proposed to modify the KNN-based systems, improving the temperature dependence of the KNN ceramics.

2. Experimental procedure

The KNN-LN-xCZ ceramics with x=0, 0.02, 0.04, 0.06, 0.08 and 0.10 were prepared by conventional solid-state reaction route. The raw materials of Na_2CO_3 (99.95%), K_2CO_3 (99%), Li_2CO_3 (99%), Nb_2O_5 (99.9%), TiO_2(99.6%) and $SrCO_3$(99%) powders were mixed by planetary mill for 24h in ethanol. This mixture was calcined at 850 °C for 6 h. After the calcinations, these powders were crushed and ball-milled again for 24h. Then, the dried powders were mixed with a polyvinyl alcohol (PVA) binder solution and then pressed into 10 mm pellets in diameter, and sintered at 1120 °C -1180 °C for 2h in ambient atmosphere. The phase structure of the samples was examined by XRD (Bruker D8 Advance, Karlsruhe, Germany) with CuKa radiation. The microstructures of samples were characterized using a scanning electron microscopy (SEM) (JSM, EMP-800; JEOL, Tokyo, Japan). To study their electrical properties, the samples were polished and painted with silver pastes on both sides and then fired at 600 °C for 30 min. The temperature dependence of the dielectric constant and loss of the samples was measured with a high-precision LCR meter (Agilent E4980A, Agilent, Palo Alto, CA). The FE hysteresis loops and strain curves of the samples were measured using a FE test system at 10Hz (Precision Premier Ⅱ; Radiant Technologies Inc, Albuquerque, NM) connected with a Miniature Plane-mirror Interferometer and the accessory Laser Interferometric Vibrometer (SP-S 120/500; SIOS Me β technik GmbH, llmenau, Germany). The samples were polarized in silicone oil under 40 kV/cm at room temperature for 30 min. The piezoelectric constant d_{33} was measured using a quasi-static d_{33} meter (IACAS ZJ-6A).

3 Results and Discussion

The phase structure of the KNN-LN-xCZ ceramics has been analyzed by combining XRD patterns and ε_r vs. T, and the detailed analysis was listed as followed. Fig.1(a) shows that all the ceramics have a pure perovskite structure without any secondary phase, confirming the complete solid solutions of ceramics. For identifying the phase transition, the expanded XRD patterns of the ceramics in the range from 44 ° to 47 ° were shown in Fig.1(b). The diffraction peak (002) is gradually rise with increasing of x content, then the two diffraction peaks (200) and (002) start to merge together at $x \geq 0.08$mol. The transition of orthorhombic phase and tetragonal phase is at the composition of $x \geq 0.04$. So the orthorhombic and tetragonal ferroelectric phases of the ceramics coexisted in the composition range of $0.04 \leq x \leq 0.08$ at room temperature. The phase boundary of orthorhombic phase transform to tetragonal phase is known as PPT to designate its difference from the MPB and PPT. For this work, the PPT composition region is $0.04 \leq x \leq 0.08$, therefore, piezoelectric and ferroelectric properties will be focused on the composition of $0.04 \leq x \leq 0.08$.

KNN-based materials have different phase transition temperature,[33] the KNN undergoes a structural phase transformation sequence on ferroelectric rhombohedral (R) $\xrightarrow{\sim -150^{\circ}C}$ ferroelectric orthorhombic (O) $\xrightarrow{\sim 210^{\circ}C}$ ferroelectric tetragonal (T) $\xrightarrow{\sim 415^{\circ}C}$ paraelectric cubic(C). The dielectric peak of the T_C can be clearly observed, and actually the T_C value is dependent on the $CaZrO_3$ content. As shown in Fig.2. the maximum dielectric constant located at the T_C increases firstly and drops dramatically, The composition with x=0 undergoes the cubic-tetragonal phase transition at 447 ^{o}C (T_C) and the tetragonal-orthorhombic phase transition at 114 ^{o}C ($T_{O\text{-}T}$), respectively. Obviously, it can be seen from Fig.2, The $T_{O\rightarrow T}$ phase is moving towards to room temperature. On the basis of these results, it can conclude that these compositions should have an orthorhombic structure at room temperature. Based on above, phase diagrams was constructed for KNN-LN-xCZ ceramics as shown in Fig.3. Three phase regions, orthorhombic, tetragonal and cubic phases are divided by T_C and $T_{O\rightarrow T}$. Both T_C and $T_{O\rightarrow T}$ were dropped with increasing of x, but T_C dropped dramatically, $T_{O\rightarrow T}$ phase is lowering towards to room temperature, from 114 ^{o}C to 25 ^{o}C. Meanwhile, d_{33} values measured at room temperature were also shown in Fig.3. With $CaZrO_3$ substitution, d_{33} increases up to 202pC/N at x=0.04, then decreased with further substitution. The enhanced piezoelectric behavior of KNN-LN-xCZ ceramics could not be simply attributed to a certain content, the new phase boundary in KNN-LN

-xCZ ceramics with $T_{O\rightarrow T}$ phase towards to room temperature acts a dominant role, in addition, the coexistence of two phases is still a necessary condition for high d_{33} valuse.

The SEM of the KNN-LN-xCZ ceramics are shown in Fig.4. For the ceramic with x=0, the grain size is from 2.5 to 3.0μm. It is noted that the grain size decreases dramatically with x increases, and more uniform grains are observed, as shown in the Fig.4(c) and (d). The result indicates that a low content of $CaZrO_3$ can well diffuse into the KNN lattices to change the phase structure, however, if the x is higher, some of $CaZrO_3$ will prohibit the grain growth.

The variations of the remanent polarization P_r and coercive field E_c with x=0, 0.04, 0.06 and 0.08 for the ceramics are shown in Fig.5. All of the KNN-LN-xCZ ceramics exhibit a well-saturated P-E loop under an electric field of about 60 kV/cm. The remnant polarization of Pr =27.2μC/cm^2 was obtained at x=0.04, which is higher than others. The high Pr is probably attributed to the domain switching and non-180^o domain contribution,[6,26] and $T_{O\rightarrow T}$ phase towards to room temperature, the polarization direction can be easily rotated by external electric fields.

It can be observed from Fig.6(a), all the sample exhibit typical butterfly shape strain curves, apparently, for x = 0.04, the total strain of 0.16% and larger negative strain of 0.025% was obtained at an electric field of 50 kV/cm, which is typical for FE material. With the increment of $CaZrO_3$ content, the strain curves show a deviation from typical FE behavior, as a result, the strain down to 0.13% for x = 0.08 with little negative strain. It can imply that a small negative strain promotes the potential for a material to display large strain response. On the other hand, the high stain value could be from the non-180^o domain contribution. As can be seen from Fig.6(b), a larger strain of

0.16% was obtained at x=0.04, which is similar to the Fig.6(a). The corresponding dynamic piezoelectric coefficient $d_{33}^{*}= S_{max}/E_{max}$, giving a maximum value of 320 pm/V at x=0.04, comparing with reported values in other KNN-based ceramics such as 310 pm/V for $K_{0.485}Na_{0.485}Li_{0.03}Nb_{0.8}Ta_{0.2}O_3$,[34] 252 pm/V for KNN modified with $LiNbO_3$,[35] reveals that KNN-LN-xCZ ceramic has a superior piezoelectric property at phase boundary. when $CaZrO_3$ was added, Ca^{2+} and Zr^{4+} were introduced into A-site and B-site, respectively, which increases the deviation displacement because the radius of Ca^{2+}(R=1.34Å, CN=12)[36,37] is smaller than that of K^{+}(R=1.64 Å, CN=12), Na^{+}(R=1.39 Å,CN=12) and the radius of Zr^{4+}(R=0.605Å, CN=6) is larger than that of Nb^{5+}(R=0.64Å, CN=6).[38] The increase of the deviation displacement gives rise to a local polar moment, leading to the formation of more macropolar domains at room temperature, meanwhile, with Ca^{2+} and Zr^{4+} replace A-site and B-site, the ionic radius become smaller and induce lattice distortion at phase boundary. Fig.1(b) has showed, diffraction peak positions shift toward the lower angle by substitution of $CaZrO_3$ until x=0.04mol, then diffraction peak positions shift toward the higher angle with increasing of $CaZrO_3$. Lattice distortion results in the shifts of diffraction peak positions, obviously, it is a transition point when x=0.04, which is in the region of PPT, just as it has been reported,[39] d_{33} at $T_{O\rightarrow T}$ affected by two phase coexistence with more polarization directions, lattice distortion affects d_{33} also. As the distortion becomes smaller toward the PPT, relatively less strain in domains switching is induced during poling and subsequently higher d_{33} is obtained because of easier better domains alignment.

As can be seen from above, it has a well performance at x=0.04, meanwhile, the properties of the KNN-LN-xCZ ceramics with x=0, x=0.04,x=0.06 and x=0.08 are summarized in Table I. Obviously, the KNN-LN-xCZ ceramics at x=0.04 exhibited outstanding performance with piezoelectric constant d_{33}=202 pC/N, d_{33}^{*}= 320 pm/V, remnant polarization of P_r =27.2μC/cm^2 and maximum strain level of 0.16% at an electric field of 50 kV/cm , which were superior to those of others. These good performances suggested that the 0.96KNN-LN-0.04CZ ceramic was a promising lead-free piezoelectric material.

4 Conclusions

Lead-free (1−x)[0.93($K_{0.5}Na_{0.5}$)NbO_3-0.07$LiNbO_3$]-x$CaZrO_3$ ternary system piezoelectric ceramics have been prepared by conventional ceramic technology, and their phase structure, microstructures and electrical properties have been investigated in details. The crystal structure of KNN-LN-xCZ ceramics was changed from orthorhombic to tetragonal at $x\geq0.04$, then both the orthogonal and tetragonal phases coexisted at $0.04<x<0.08$, and was converted to tetragonal structure at $x>0.08$. The Curie temperature decreased with increasing of $CaZrO_3$ content. At phase boundary, the maximum value d_{33}=202 pC/N and d_{33}^* of 320 pm/V was obtained at x=0.04. Curie temperature T_c=350°C, strain levels of 0.16% at 50 kV/cm and remnant polarization P_r =27.2μC/cm^2. The polymorphic phase transition between the orthorhombic and tetragonal phases plays a very important role in enhancement of the piezoelectric properties of KNN-LN-xCZ ceramics. These good performances suggested that the KNN-LN-xCZ ceramic was a promising lead-free piezoelectric material.

Acknowledgements

The authors would like to acknowledge the National Natural Science Foundation of China under Grant No. 51372171, 51332003, and the Shanghai Municipal Natural Science Foundation under Grant No.12ZR1434600.

Notes and references

[1] G.H. Haertling, *J. Am .Ceram .Soc.*, 1999, 82, 797–818.

[2] D.E. Cox, B. Noheda, G. Shirane, Y. Uesu, K. Fujishiro, Y. Yamada, *Appl. Phys. Lett.*, 79 (2001) 400.

[3] Deepam Maurya, A. Pramamick, M. Feygenson, et al., *J. Mater. Chem. C*, 2014,2,8423-8431.

[4] Y. Saito, H. Takao, T. Tani, T. Nonoyama, K. Takatori, T. Homma, T. Nagaya, M. Nakamura, *Nature*, 2004, 432, 84–87.

[5] Pil Gu Kang, Byung Kil Yun, Kil Dong Sung, et al., *RSC Adv*., 2014, 4, 29799.

[6] G. Viola, T Saunders, X. Wei, K. B. Chong, H. Luo, M. J. Reece and H. Yan, *J. Adv. Dielect.* 2013, 3, 1350007

[7] D. Maurya, Y. Zhou, Y Yan and S. Priya, *J. Mater. Chem. C*, 2013, 1, 2102-2111

[8] Elena Aksel, Jacob L. Jones, *Sensors*, 2010, 10, 1935-1954.

[9] J. G. Wu, *RSC Adv*., 2014, 4, 53490.

[10] F. Z. Yao, Q. Yu, K. Wang, Q. Li and J. F. Li, *RSC Adv*., 2014, 4, 20062.

[11] Jing-Feng Li, Yuhua Zhen, Bo-Ping Zhang, Li-Min Zhang, *Ceram. Int.*, 2008, 34,783–786

[12] H. Du, F. Tang, F. Luo, D. Zhu, S. Qu, Z. Pei, W. Zhou, *Mater. Res. Bull.*, 2007, 42, 1594–1601.

[13] Zhen Y, Li J F. *J. Am .Ceram .Soc.*, 2006, 89, 3669-3675.

[14] Z. Shen, Y. Li, L. Jiang, *J Mater Sci-Mater El.* 2011, 22, 1071–1075.

[15] Chee Kiang Ivan Tan, and Kui Yao, *J. Am. Ceram. Soc.* 2011, 94, 776–781.

[16] B. Zhang, J. Wu, X. Cheng.et al., *ACS Appl. Mater. Inter.*, 2013, 5, 7718-7725.

[17] M. Matsubara, K. Kikuta, S. Hirano, *Jpn. J. Appl. Phys.* 2005, 44, 6618–6623.

[18] Y. Guo, K. Kakimoto, H. Ohsato, *Appl. Phys. Lett*. 2004, 85, 4121–4123.

[19] P. Kumar, P. Palei, *Ceram Int.*, 2010, 36, 1725–1729.

[20] S.J. Zhang, R. Xia, T.R. Shrout, G.Z. Zang, J.F. Wang, *J. Appl. Phys*. 2006, 100, 104108.

[21] J.-F. Li, K. Wang, B.-P. Zhang, L.M. Zhang, *J. Am. Ceram. Soc.*, 2006, 89, 706–709.

[22] E. Hollenstein, M. Davis, D. Damjanovic and N. Setter, *Appl. Phys. Lett.*, 2005, 87, 182905.

[23] J. L. Zhang, X. J. Zong, L. Wu, Y. Gao, P. Zheng, and S. F. Shao, *Appl. Phys. Lett.*,2009, 95, 022909.

[24] T. A. Skidmore, T. P. Comyn and S. J. Milne, *Appl. Phys. Lett.*, 2009, 94, 222902.

[25] Y. Chang, Z. Yang, D. Ma, Z. Liu, and Z. Wang, *J. Appl. Phys.*, 2009, 105, 054101.

[26] H. Yan, F. Inam, G. Viola, et al., *J. Adv. Dielect.*, 2011, 1, 107-118.

[27] D. Maurya, A. Kumar, V. Petkov, et al., *RSC Adv.*, 2014.4.1283-1292.

[28] Deepam Maurya, M. Murayama, A. Pramanick, W. T. Reynolds Jr, Ke An and Shashank Priya, *J. Appl. Phys.*, 2013, 113, 114101.

[29] D.E. Cox, B. Noheda, G. Shirane, Y. Uesu, K. Fujishiro, Y. Yamada, *Appl. Phys. Lett.*, 2001, 79, 400.

[30] T. Huang, D.Q. Xiao, C. Liu, F.X. Li, B. Wu, J.G. Wu, J.G. Zhu, *Ceram. Int.*, 2014, 40, 2731–2735.

[31] Y. Guo, K. I. Kakimoto and H. Ohsato, *Appl. Phys. Lett.*, 2004, 85, 4121-3.

[32] F. Z. Yao, Eric A. Patterson, Ke Wang, Wook Jo, Jürgen Rödel and J.F. Li, *Appl. Phys. Lett.*, 2014, 104, 242912.

[33] Wenwei Ge, Jiefang Li, and D. Viehland, *Phys. Rev. B*, 2011, 83, 224110.

[34] E. Hollenstein, M. Davis, D. Damjanovic, N. Setter, *Appl. Phys. Lett.*, 2005, 87, 182905–182908.

[35] E. Li, R. Suzuki, T. Hoshina, H. Takeda, T. Tsurumi, *Appl. Phys. Lett.*, 2009, 94, 132903–132905.

[36] Du H, Zhou W, Zhu D, et al., *J. Am .Ceram .Soc.*, 2008, 91, 2903-2909.

[37] Shannon R D, *Acta Cryst.*, 1976, A32, 751.

[38] Bobnar, J. Bernard, and M. Kosec, *Appl. Phys. Lett.*, 2004, 85, 994.

[39] Y. S. Sung, J. M. Kim, J. H. Cho, T. K. Song, M. H. Kim and T. G. Park., *Appl. Phys. Lett.*, 2010, 96, 202901.

Figures and captions

Fig.1. XRD patterns of the KNN-LN-xCZ ceramics in the 2θ range of (a) 20 °–60 ° and (b) 44 °–47 °, respectively.

Fig.2. Temperature dependence of the dielectric constant and dielectric loss of the KNN-LN-xCZ ceramics measured at10kHz in the temperature range from room temperature to 550^{o}C .

Fig.3. Phase diagrams (T_C and $T_{\mathrm{O}\rightarrow\mathrm{T}}$) of the KNN-LN-xCZ ceramics showing the difference caused by $CaZrO_3$ substitution, d_{33} also shown at room temperature

Fig.4. SEM of the ceramics with (a) x = 0, (b) x = 0.04, (c)x = 0.06, and (d) x =0.08 sintered at 1160 ℃ for 2h

Fig.5. *P*-*E* hysteresis loops of the KNN-LN-xCZ ceramics (inset shows *I*-*E* curves)

Fig.6. S–E curves of the KNN-LN-xCZ ceramics measured at 10Hz and room temperature for (a) bipolar strain and (b) unipolar strain.

Fig.1

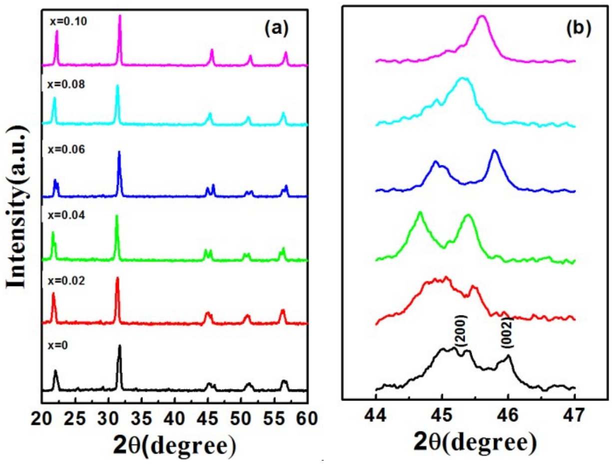
(a)
(b)
x=0.10
x=0.08
x=0.06
x=0.04
x=0.02
x=0
Intensity(a.u.)
20 25 30 35 40 45 50 55 60
2θ(degree)
(200)
(002)
44 45 46 47
2θ(degree)

Fig.2

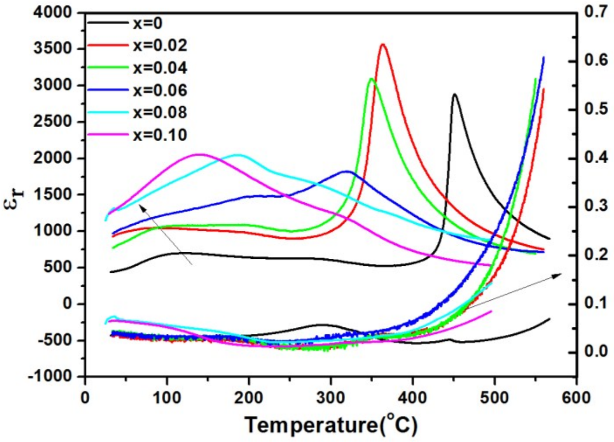
x=0
x=0.02
x=0.04
x=0.06
x=0.08
x=0.10
ε_r
4000
3500
3000
2500
2000
1500
1000
500
0
-500
-1000
0.7
0.6
0.5
0.4
0.3
0.2
0.1
0.0
0
100
200
300
400
500
600
Temperature(°C)

Fig.3

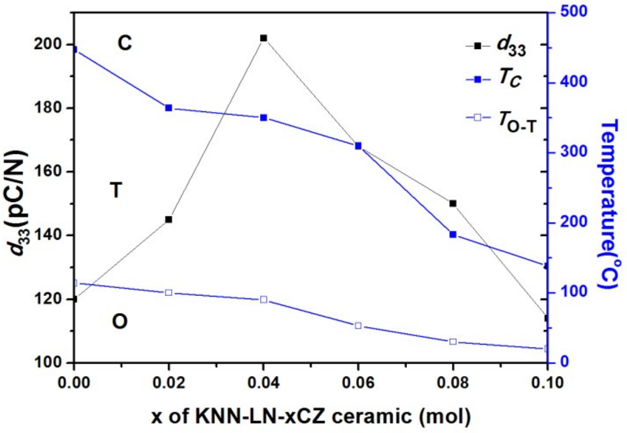
C
T
O
d_{33}
T_C
$T_{O\text{-}T}$
d_{33}(pC/N)
200
180
160
140
120
100
Temperature(°C)
500
400
300
200
100
0
0.00
0.02
0.04
0.06
0.08
0.10
x of KNN-LN-xCZ ceramic (mol)

Fig.4

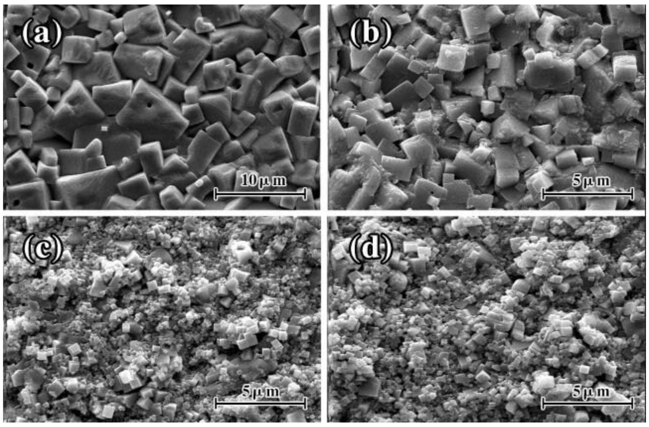

Fig.5

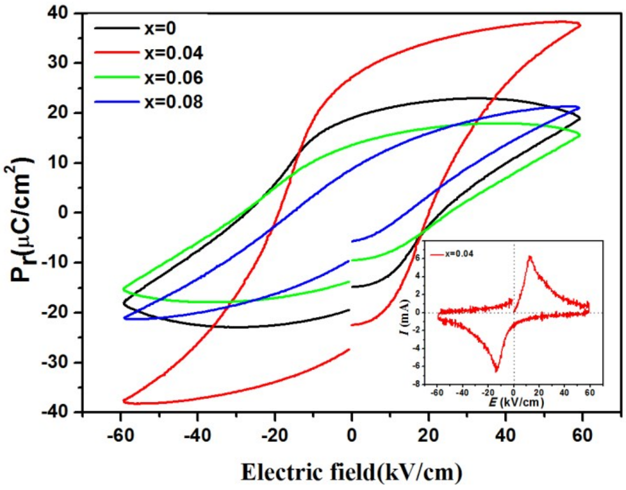
x=0
x=0.04
x=0.06
x=0.08
$P_r(\mu C/cm^2)$
40
30
20
10
0
-10
-20
-30
-40
-60
-40
-20
0
20
40
60
Electric field(kV/cm)
x=0.04
I (mA)
6
4
2
0
-2
-4
-6
-8
-60
-40
-20
0
20
40
60
E (kV/cm)

Fig.6

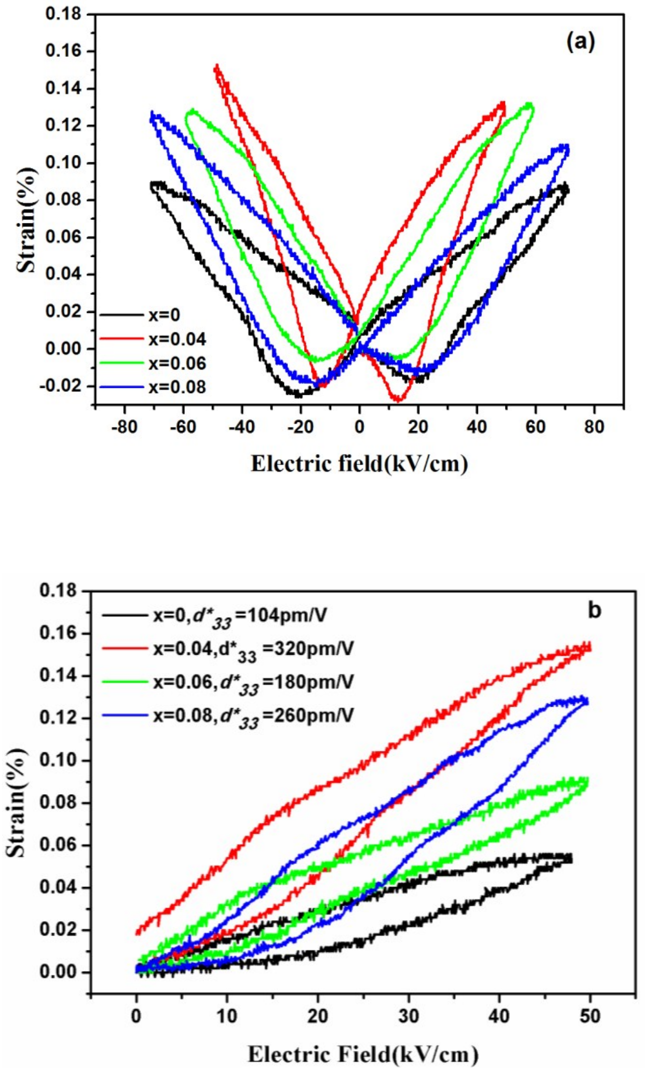
(a)
Strain(%)
0.18
0.16
0.14
0.12
0.10
0.08
0.06
0.04
0.02
0.00
-0.02
-80
-60
-40
-20
0
20
40
60
80
Electric field(kV/cm)
x=0
x=0.04
x=0.06
x=0.08
b
x=0,d*33=104pm/V
x=0.04,d*33 =320pm/V
x=0.06,d*33=180pm/V
x=0.08,d*33=260pm/V
Strain(%)
0.18
0.16
0.14
0.12
0.10
0.08
0.06
0.04
0.02
0.00
0
10
20
30
40
50
Electric Field(kV/cm)

Table I. Piezoelectric and dielectric properties of the KNN-LN-xCZ ceramics with x=0, x=0.04, x=0.06, x=0.08

	d_{33} (pC/N)	d_{33}^* (pm/V)	*Tc* (℃)	tanδ (%)	*Pr* (μC/cm^2)	ε_r (25℃)	Strain (%)
X=0	120	104	447	0.036	18.8	2880	0.05
X=0.04	202	320	350	0.038	27.2	3083	0.16
X=0.06	168	180	310	0.045	14.3	1806	0.09
X=0.08	150	260	183	0.07	8.7	2043	0.13